Electronic Supporting Information

Hybrid Organic Nanocrystal/Carbon Nanotube Film Electrodes for Air- and Photo-Stable Perovskite Photovoltaics

Raja Bhaskar Kanth Siram[1,2§], Mark V. Khenkin[3§], Angelica Niazov-Elkan[1], Anoop K.M.[3], Haim Weissman[1], Eugene A. Katz[3,4*], Iris Visoly-Fisher[3,4*] and Boris Rybtchinski[1*]

[1]Department of Organic Chemistry, Weizmann Institute of Science, Rehovot 76100, Israel

[2]Department of Chemistry, School of Science, Gitam University (deemed to be university), Rudraram, Hyderabad 502329, India

[3]Dept. of Solar Energy and Environmental Physics, Swiss Inst. for Dryland Environmental and Energy Research, J. Blaustein Institutes for Desert Research, Ben-Gurion University of the Negev, Midreshet Ben-Gurion 8499000, Israel

[4]Ilse Katz Institute for Nanoscale Science and Technology, Ben-Gurion University of the Negev, Be'er-Sheva 8410501, Israel

§RBKS and MVK contributed equally

*Corresponding authors: Boris.Rybtchinski@weizmann.ac.il, keugene@bgu.ac.il, irisvf@bgu.ac.il

Experimental Section:

Materials: Fluorine-doped tin oxide coated glass (FTO) TCO-XY15, 15Ω/sq was purchased from Xinyan Technology Ltd. Cesium bromide (99.999%), lead bromide (98%), titanium diisopropoxide bis(acetylacetonate) (75 wt. % in isopropanol), Multiwall carbon nanotubes (MWCNT, average diameter of 9.5 nm and 1.5 µm length) and anhydrous dimethyl formamide (DMF, 99.8%) were purchased from Sigma-Aldrich. The materials were used as purchased. Mesoporous TiO_2 paste was purchased from Dyesol. It was diluted to 2:7 weight ratio with ethanol and sonicated for about 30 min to obtain the homogenuous dispersion. Conductive carbon paste was received from SPI supplies with the catalog no. Z05006.

Structural characterization: SEM images were taken using a Zeiss ULTRA high-resolution microscope. For cross-sectional images the samples were cleaved.

UPS measurements were carried out with a Kratos AXIS ULTRA system, using a concentric hemispherical analyzer for photo-excited electron detection. UPS was measured with a helium discharge lamp, using the He I (21.22 eV) and He II (40.8 eV) radiation lines. Total energy resolution was less than 100 meV, as determined from the Fermi edge of a Au reference sample. All UPS spectra were measured with a -10 V bias applied to the sample to observe the photoemission onset at low kinetic energies.

Hybrid CNT film fabrication: 2 mg of nitro-substituted PDI derivative (ONC**1**) or unsubstituted PDI was taken in a 20 mL vial and added equal amount of MWCNTs and 20 mL of water:THF=7:3 (v/v) solution. The mixture was sonicated for 45-60 min to disperse the MWCNTs fully n. The solution was centrifuged at 3000 rpm for 5 min to remove the undispersed MWCNTs. The supernatant was filtered through a PTFE membrane under argon pressure of 2 bar. ONC**2**•MWCNT films were prepared in a similar fashion. The films were dried under vacuum overnight and detached from the membrane to give the free-standing hybrid ONC•MWCNT films.

$CsPbBr_3$ perovskite solar cell fabrication: F-doped tin oxide (FTO) transparent conducting substrates were cleaned by sequential sonication in warm aqueous alconox solution, deionized water, acetone, and ethanol for 20 min. The cleaned substrates were dried in a N_2 stream. A compact TiO_2 layer (~30 nm) was applied on the clean FTO substrates by spray pyrolysis of a 20 mM titanium diisopropoxide bis(acetylacetonate) solution in isopropanol, using air as the carrier gas, on a hot plate set to 350 °C, followed by annealing at 500 °C for 1 h in air. A 400-450 nm thick mesoporous TiO_2 layer was deposited by spin casting a TiO_2 paste onto the compact TiO2 layer. These substrates were calcinated at 500 °C in air. The substrates were cooled to room temperature and used for the perovskite layer deposition. The perovskite layer was deposited by a 2-step technique at an ambient atmosphere:[1] 1M solution of $PbBr_2$ in dimethyl formamide (DMF) was strirred at 70 °C for about 20 min. This solution was filtered through 0.2 μm PTFE filter and used immediately. The solution was spin-casted on preheated substrates at 75 °C for 2 min at 2500 rpm and was heated on hot plate at 75 °C for 30 min. After cooling the substrates were dipped in a hot solution of 17 mg/mL CsBr in methanol for 10 min. Then the substrates were washed with propanol followed by drying under N_2 stream and annealed for 10 min at 250 °C. The samples were left overnight in the dark in dry air before deposition of the top electrode. For control samples, ~100-nm thick gold contacts were thermally evaporated through a shadow mask (with area 0.24 cm^2).

Deposition of Hybrid Membrane: The free-standing hybrid MWCNT film was wetted with acetonitrile and transferred onto the perovskite layer carefully. The solvent was evaporated by heating at 70 °C for about 1 min in air.

Solar cell device characterization: The current-voltage curves of the devices were measured with a Keithley 2400-LV SourceMeter and controlled with a Labview-based, in-house written program. A home-built solar simulator equipped with a xenon arc lamp and AM1.5 filter whose power output was adjusted to match AM 1.5 global sunlight (100 mW/cm^2) by using a reference Si photodiode (IXOLARTM High Efficiency SolarBIT, IXYS KXOB22-12X1L) as well as by calibrating against natural sunlight measured by an Eppley pyranometer was used for illumination. The device was characterized through a 0.16 cm^2 mask.

The EQE of the devices was measured using a Thermo Oriel monochromator with the light chopped at 10 Hz. The current was measured by an Oriel Merlin and TTI PDA-700

---

[1] M. Kulbak, D. Cahen, G. Hodes, *J. Phys. Chem. Lett.* 2015, **6**, 2452-2456.

photodiode amplifier. The EQE was calculated by referencing to the spectral response of a Si photodiode with a known EQE. Photocurrent density (J_{SC}^{calc}) was determined from EQE measurements by integrating the product of the measured spectral EQE and the number of incident photons (N_p) at each wavelength (λ) over the whole spectral range, typically with an AM 1.5G solar spectrum:

$$J_{sc}^{calc} = \int q \, EQE(\lambda) \, N_p(\lambda) \, d\lambda \, .$$

Device stability studies: To demonstrate the effect of hybrid ONC1•MWCNT electrodes on the device stability the cells were aged in following conditions: 1) “on-shelf” (25 °C; 25-35% relative humidity; in the dark); 2) at elevated temperatures (60 °C; in air in the dark); 3) under continuous illumination (simulated sunlight; 100 mW/cm^2; in air; at open circuit); 4) outdoor. Overall, over 25 cells were used for stability studies.

Outdoor degradation experiments were performed in Sede Boqer, Israel (Lat. 30.8°N, Lon. 34.8°E, Alt. 475 m) following the ISOS-O-1 protocol[2] in February-May 2017. The sunlight spectrum measured at noontime ± 2–3 hours at Sede Boqer is very close to the AM1.5G spectrum.[3] The devices mounted on a fixed angle (30°) stand were exposed to natural sunlight at open circuit during daytime (from 10:00 to 17:00) and kept in the dark in a desiccant box at night. Weather conditions during the experiment are shown in Fig. S14. The *J-V* curves during stability studies were measured with a Keithley 2401 source meter under the illumination of an AAA class Oriel VeraSol LSS-7120 solar simulator (67 mW/cm^2). The voltage sweeps were performed in the range -0.2 to 1.5 V in forward and reverse sweep directions with a scanning rate of ~40 mV/s. No preconditioning was applied before measurements. 6 cells with hybrid ONC1/MWCNT and 5 cells with standard gold electrodes were tested in outdoor studies.

---

[2] M. O. Reese *et al.*, *Sol. Energy Mater. Sol. Cells* 2011, **95**, 1253-1267.

[3] D. Berman, D. Faiman. *Sol. Energy Mater. Sol. Cells* 1997, **45**, 401-412.

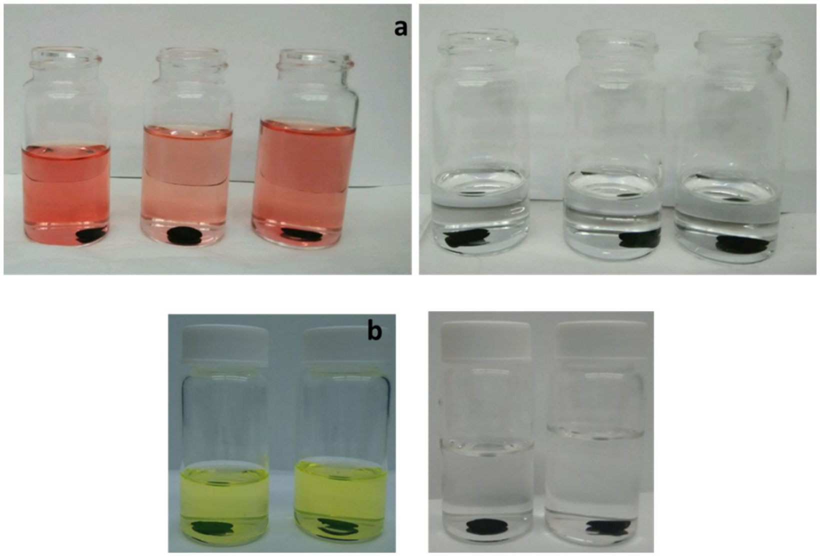

Figure S1: Dissolution of a) NO_2-EP-PDI crystals (ONC**1**) in acetone b) EP-PDI crystals (ONC**2**) in chloroform (washing ONCs from the hybrid MWCNT membrane).

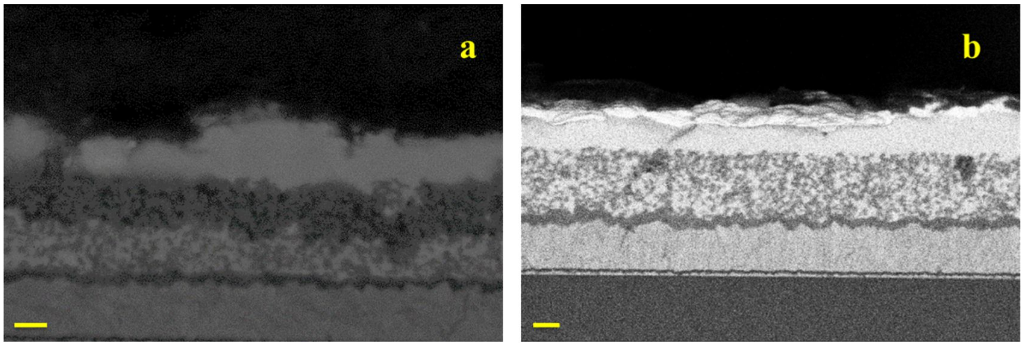

Figure S2: cross-sectional SEM images a) FTO/d-TiO_2/mp-TiO_2/$CsPbBr_3$/Hybrid MWCNT electrode b) FTO/d-TiO_2/mp-TiO_2/$CsPbBr_3$/Au electrode with Back scattered detector. Scale bar is 200 nm.

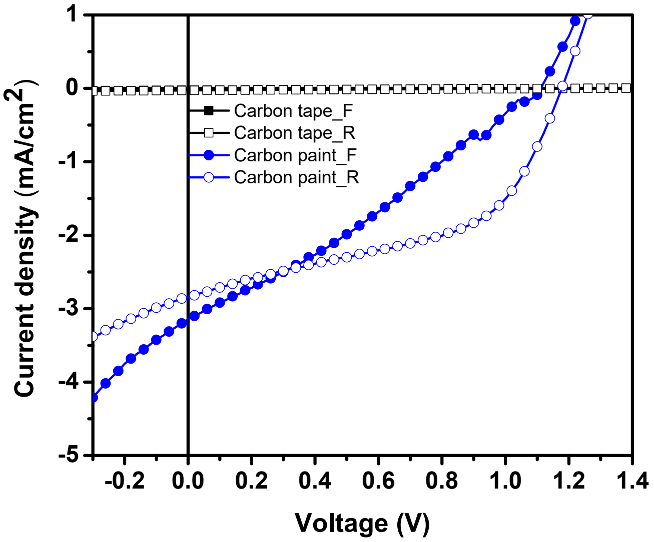

Figure S3: J-V characteristics of FTO/d-TiO_2/mp-TiO_2/$CsPbBr_3$/carbon tape or carbon paint as electrode devices. Filled circle – forward scan and empty circle – reverse scan.

	Carbon Tape		**Carbon Paint**	
	FS	**RS**	**FS**	**RS**
V_{oc} (Volts)	1.24	1.24	1.11	1.18
J_{sc} (mA/cm^2)	0.11	0.13	3.15	2.84
Fill Factor (FF)	0.32	0.29	0.29	0.49
PQE (%)	0.04	0.04	1.01	1.65

Table S1: J-V characteristics of $CsPbBr_3$ perovskite solar cells with carbon tape or carbon paste as back electrode.

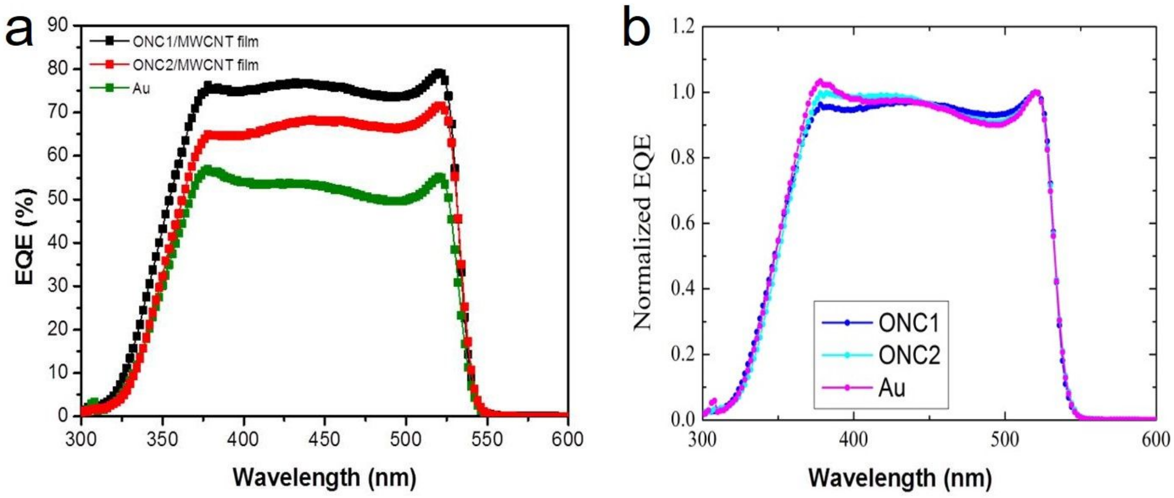

Figure S4. (a) EQE spectra measured with FTO/d-TiO$_2$/mp-TiO$_2$/CsPbBr$_3$/back electrode, where the back electrode was ONC1•MWCNT, ONC2•MWCNT or Au. (b) The same normalized to the value at 450 nm.

Electrode	**J_{SC}**	**J_{SC}^{calc}**
Au	4.341	4.297
ONC**1**/MWCNT	6.171	6.184
ONC**2**/MWCNT	5.732	5.527

Table S2. Comparison of short circuit current densities of CsPbBr$_3$ solar cells with different back contacts from J-V and EQE measurements.

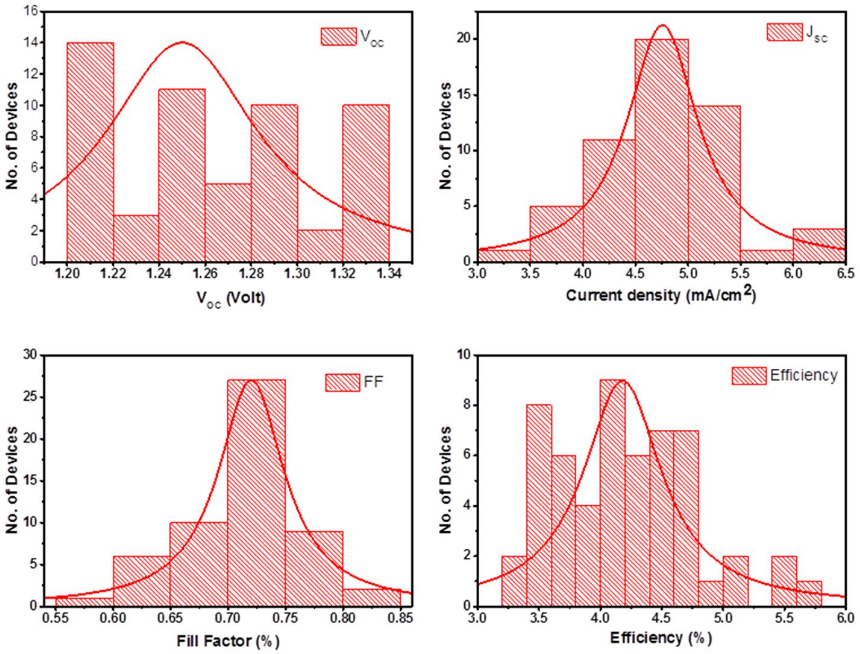

Figure S5: Histograms of PV parameters of FTO/d-TiO_2/mp-TiO_2/$CsPbBr_3$/Hybrid MWCNT electrode.

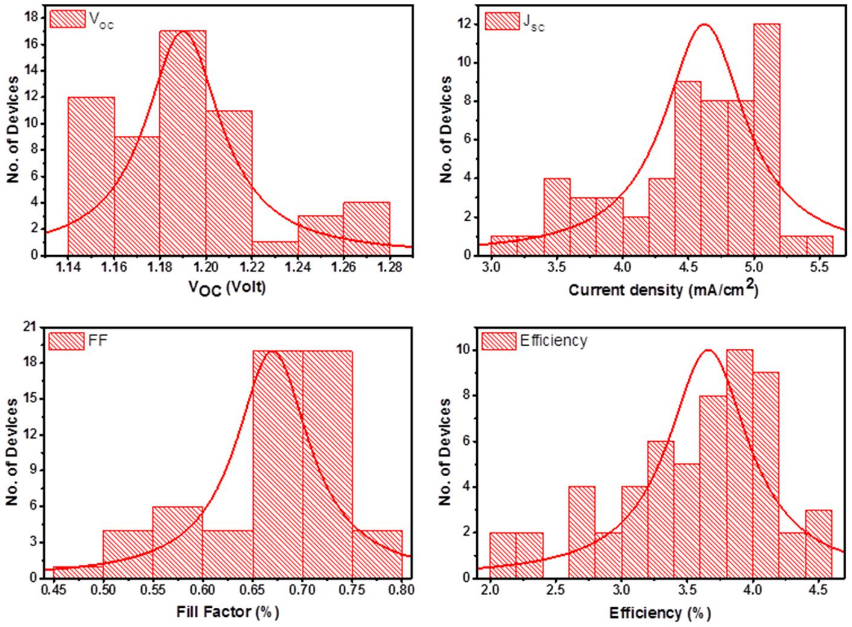

Figure S6: Histogram of PV parameters of FTO/d-TiO_2/mp-TiO_2/$CsPbBr_3$/Au electrode.

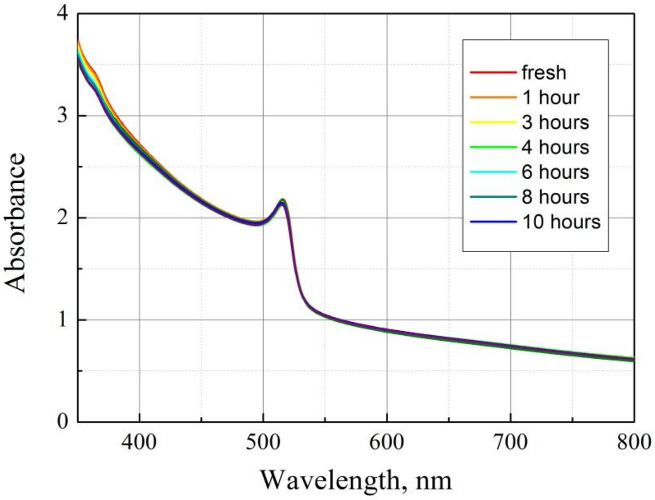

Figure S7: Absorption spectra of $CsPbBr_3$ film after exposure to concentrated sunlight with intensity of 100 suns.

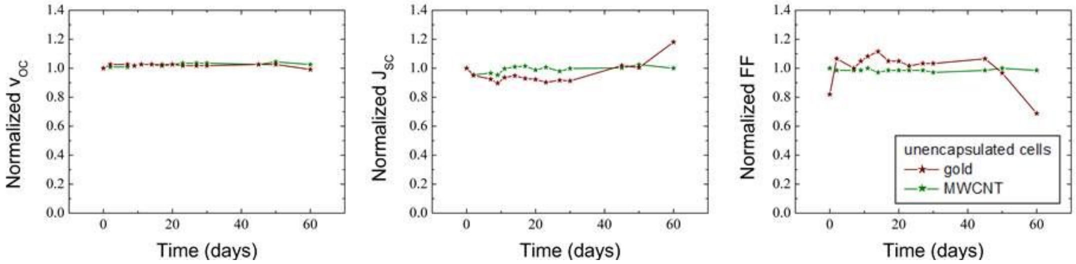

Figure S8: “On-shelf” stability studies of FTO/d-TiO_2/mp-TiO_2/$CsPbBr_3$/Hybrid MWCNT electrode devices.

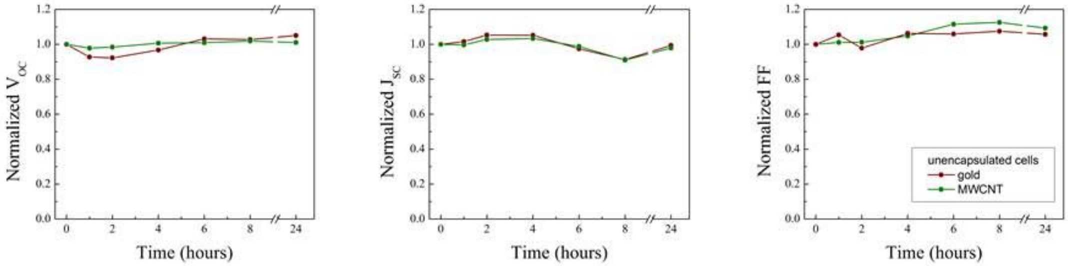

Figure S9: Thermal stability of principal PV parameters of FTO/d-TiO_2/mp-TiO_2/$CsPbBr_3$/Hybrid MWCNT and gold electrode devices.

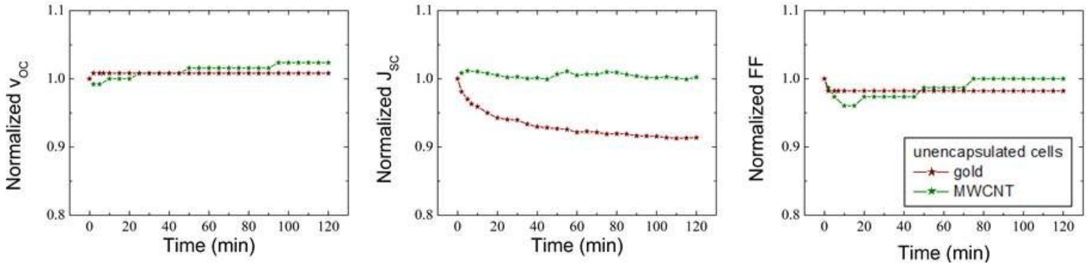

Figure S10: Photo-stability under continuous illumination of principal PV parameters of FTO/d-TiO_2/mp-TiO_2/$CsPbBr_3$/Hybrid MWCNT and gold electrode devices.

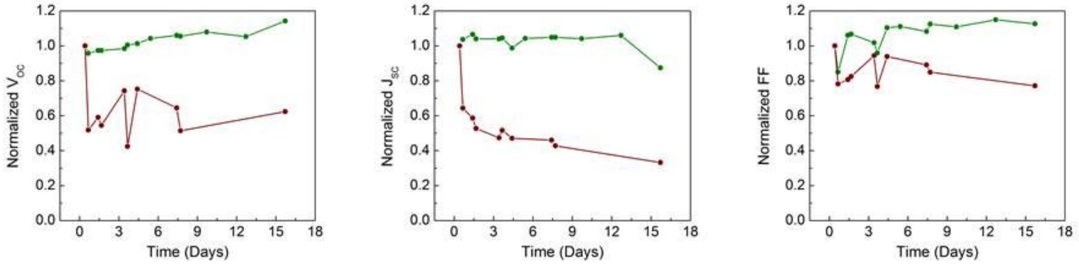

Figure S11: Outdoor stability of principal PV parameters of FTO/d-TiO_2/mp-TiO_2/$CsPbBr_3$/Hybrid MWCNT and gold electrode devices.

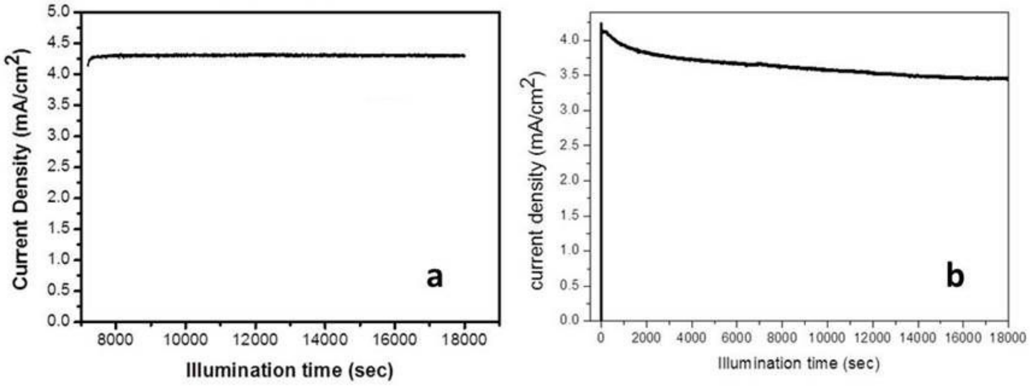

Figure S12. Current density evolution upon MPP tracking of (a) FTO/d-TiO_2/mp-TiO_2/$CsPbBr_3$/Hybrid MWCNT and (b) gold electrode devices.

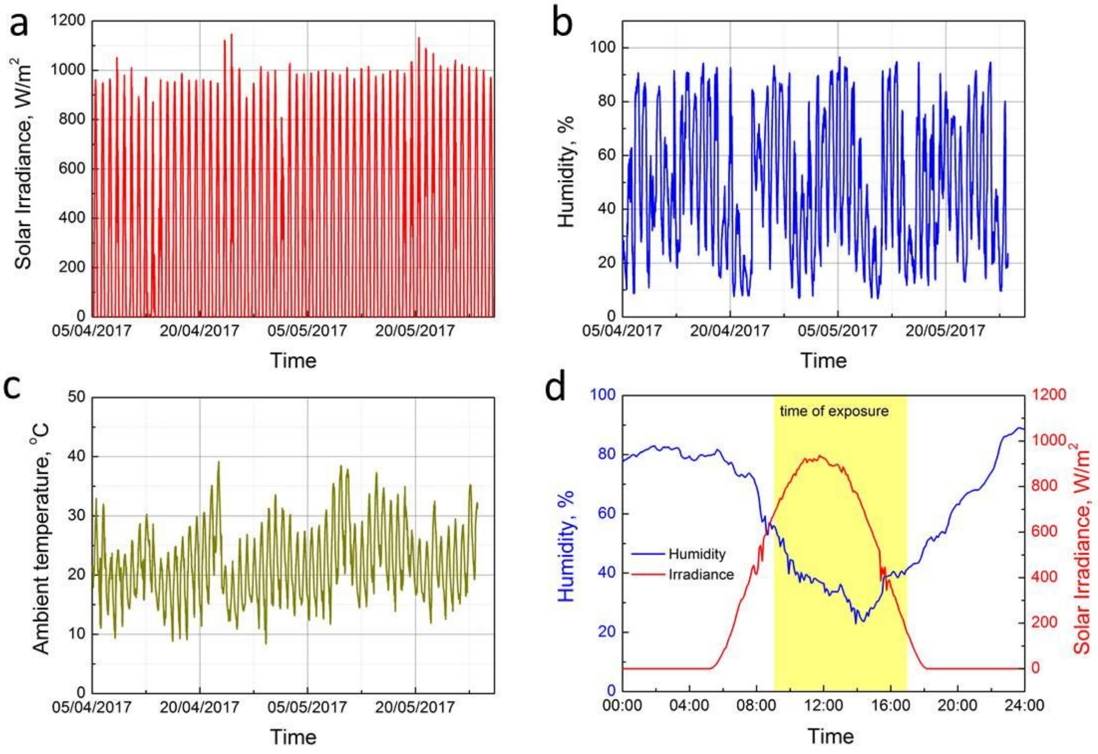

Figure S13: Solar irradiance (a), humidity (b) and temperature (c) in Sede Boqer during the outdoor experiment shown in Figure 6. Panel d shows hourly resolved solar irradiance and humidity during one day.

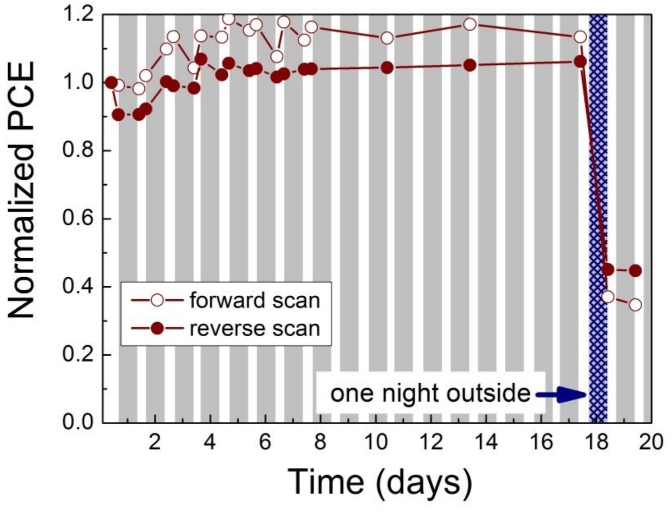

Figure S14: The PCE evolution of MWCNT device with day-night cycle during outdoor exposure. The gray areas correspond to nighttime, during which the cells were kept in a desiccant box in the dark. The dramatic degradation on the day 18 is a result of one night outdoor, likely, due to morning dew.

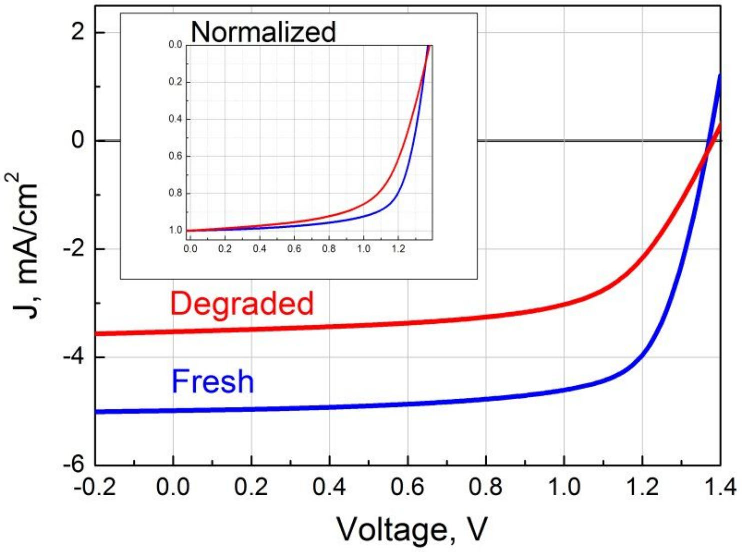

Figure S15: The J-V curves of the PSC before and after outdoor aging experiment shown in Figure. 6. The inset shows the same curves normalized to the J_{SC} value.